



# UAV LiDAR Metrics for Monitoring Crop Height, Biomass and Nitrogen Uptake: A Case Study on a Winter Wheat Field Trial

Christoph Hütt<sup>1</sup>  · Andreas Bolten<sup>1</sup> · Hubert Hüging<sup>2</sup> · Georg Bareth<sup>1</sup>

Received: 6 April 2022 / Accepted: 23 November 2022 / Published online: 14 December 2022  
© The Author(s) 2022

## Abstract

Efficient monitoring of crop traits such as biomass and nitrogen uptake is essential for an optimal application of nitrogen fertilisers. However, currently available remote sensing approaches suffer from technical shortcomings, such as poor area efficiency, long postprocessing requirements and the inability to capture ground and canopy from a single acquisition. To overcome such shortcomings, LiDAR scanners mounted on unmanned aerial vehicles (UAV LiDAR) represent a promising sensor technology. To test the potential of this technology for crop monitoring, we used a RIEGL Mini-VUX-1 LiDAR scanner mounted on a DJI Matrice 600 pro UAV to acquire a point cloud from a winter wheat field trial. To analyse the UAV-derived LiDAR point cloud, we adopted LiDAR metrics, widely used for monitoring forests based on LiDAR data acquisition approaches. Of the 57 investigated UAV LiDAR metrics, the 95th percentile of the height of normalised LiDAR points was strongly correlated with manually measured crop heights ( $R^2=0.88$ ) and with crop heights derived by monitoring using a UAV system with optical imaging ( $R^2=0.92$ ). In addition, we applied existing models that employ crop height to approximate dry biomass (DBM) and nitrogen uptake. Analysis of 18 destructively sampled areas further demonstrated the high potential of the UAV LiDAR metrics for estimating crop traits. We found that the bincentile 60 and the 90th percentile of the reflectance best revealed the relevant characteristics of the vertical structure of the winter wheat plants to be used as proxies for nitrogen uptake and DBM. We conclude that UAV LiDAR metrics provide relevant characteristics not only of the vertical structure of winter wheat plants, but also of crops in general and are, therefore, promising proxies for monitoring crop traits, with potential use in the context of Precision Agriculture.

**Keywords** 3D modelling · LiDAR metrics · Precision agriculture · Crop trait · Fertilisation · Biomass · Nitrogen

## Zusammenfassung

Eine effiziente Überwachung von Pflanzenmerkmalen wie Biomasse und Stickstoffaufnahme ist essentiell für einen optimalen Einsatz von Stickstoffdünger. Die derzeit verfügbaren Fernerkundungsmethoden weisen jedoch Mängel auf. In diesem Zusammenhang stellen LiDAR-Scanner, montiert auf unbemannten Luftfahrzeugen (UAV), eine vielversprechende Sensortechnologie dar. Um das Potenzial von UAV LiDAR für das Monitoring von Feldfrüchten zu testen, wurde mit einem RIEGL Mini-VUX-1 LiDAR-Scanner, montiert auf dem UAV DJI Matrice 600 pro, ein Feldversuch mit Winterweizen überflogen. Zur Analyse der dabei aufgenommenen UAV LiDAR Punktwolke haben wir LiDAR-Metriken verwendet, die für Analysen von Waldbeständen weit verbreitet sind. Von den 57 untersuchten UAV LiDAR-Metriken korrelierte das 95. Perzentil der Höhe der normierten LiDAR-Punkte stark mit terrestrisch gemessenen Pflanzenhöhen ( $R^2=0.88$ ) und mit Pflanzenhöhen, die durch multitemporales Monitoring mit dem optischen UAV-System Phantom 4 RTK ermittelt wurden ( $R^2=0.92$ ). Weiterhin

---

✉ Christoph Hütt  
christoph.huett@uni-koeln.de

<sup>1</sup> GIS & RS Group, Institute of Geography, University of Cologne, Albertus-Magnus-Platz, 50923 Cologne, Germany

<sup>2</sup> INRES, Institute of Crop Science and Resource Conservation, University of Bonn, Katzenburgweg 5, 53115 Bonn, Germany

haben wir bereits existierende Modelle angewandt, die die Pflanzenhöhe zur Abschätzung der trockenen Biomasse (DBM) und der Stickstoffaufnahme verwenden. Die Analyse von 18 destruktiv beprobten Flächen bestätigte weiterhin das hohe Potenzial der UAV LiDAR Metriken für die Abschätzung von Pflanzenmerkmalen. Das Bincentile 60 und das 90. Perzentil der Pflanzenreflexion stellten sich als relevante Merkmale heraus, um aus der 3D- Punktwolke der Winterweizenpflanzen die Stickstoffaufnahme und die DBM abzuleiten. Wir kommen zu dem Schluss, dass UAV LiDAR-Metriken relevante Merkmale der vertikalen Struktur von Winterweizenpflanzen, aber auch von Nutzpflanzen im Allgemeinen, zeigen können und daher eine vielversprechende Anwendung für die Überwachung von Pflanzenmerkmalen sind, mit potentielltem Einsatz im Rahmen von Präzisionslandwirtschaft.

## 1 Introduction

In precision agriculture, remote sensing plays a crucial role in monitoring crop parameters to improve nitrogen fertilisation (Heege et al. 2008; Huang et al. 2015; Mulla 2013). An optimised application of nitrogen maximises yields and minimises environmental impacts such as eutrophication, nitrate leaching or greenhouse gas emissions (Ju et al. 2009; Wilson et al. 2015). Hence, the nitrogen nutrition index (NNI) was developed as a conceptual approach to identify optimum nitrogen application rates during crop growth to improve nitrogen use efficiency (Gastal and Lemaire 2002; Lemaire et al. 2008).

The NNI can be calculated using dry biomass and nitrogen concentration in a given phenological stage and knowing the nitrogen dilution effect by developing a critical nitrogen dilution curve for each crop (Huang et al. 2015). Therefore, remote sensing approaches target the non-destructive estimation of both parameters, dry biomass and nitrogen concentration. For nitrogen concentration, optical sensors (multi- or hyperspectral) can be utilised (Hansen and Schjoerring 2003; Li et al. 2010). For the determination of crop biomass, Remote Sensing-derived crop height can be utilised (Bendig et al. 2013, 2014; Hoffmeister et al. 2010). To derive crop height, three different remote sensing approaches are applied: (i) ultrasonic, (ii) Structure from Motion (SfM) and (iii) laserscanning.

(i) Ultrasonic devices, mainly mounted on tractors, are used as a remote sensing method to derive crop height and to estimate biomass. Crop height measured by ultrasonic devices has been shown to generate reliable estimates of biomass for many crops (Barmeier et al. 2016; Pittman et al. 2015). However, ultrasonic sensors are to sense distances of up to five metre and are usually mounted on tractors for crop monitoring. In addition, ultrasonic sensors can only produce point measurements (Schirrmann et al. 2017) and cannot provide spatially continuous raster data.

(ii) In contrast, UAV-derived image data can be utilised for SfM providing continuous raster data of crop height. By subtracting a digital terrain model (DTM) from the digital surface model (DSM) of the crop canopy surface in a

Geographic Information System (GIS) environment, absolute crop height in metres, with centimetre precision can be derived. Numerous studies have demonstrated that UAV-derived crop height is a robust estimator for crop biomass as shown, e.g. in the case of barley (Bendig et al. 2014), wheat (Jenal et al. 2021), maize (Niu et al. 2019), and poppy (Iqbal et al. 2017).

(iii) Finally, light detection and ranging (LiDAR) (also known as laserscanning) is an active remote sensing method. LiDAR directly generates 3D point clouds, which can be analysed to determine crop height. Crop height derived by terrestrial laserscanning (TLS) proved to be a robust estimator for biomass (Hoffmeister et al. 2016; Tilly et al. 2014). Nevertheless, TLS is labour intensive, and the scanned area per day is less than 20 ha. Furthermore, airborne laserscanning (ALS) campaigns using manned aircrafts are very costly and require extensive preparation. In contrast, UAV LiDAR is more flexible, cost- and area effective. Although the use of UAV LiDAR for crop monitoring is still in its infancy, existing studies indicate that this approach has a high potential for estimating crop traits such as density (Bates et al. 2021), biomass (ten Harkel et al. 2019), and height (Zhang et al. 2021).

The existing studies on UAV LiDAR crop trait estimation use self-developed complex algorithms that have to be adapted to the respective application (e.g. 3DPI; ten Harkel et al. 2019). However, LiDAR has been very successfully used for forest studies and inventories (Bouvier et al. 2015). The state-of-the-art approach is to estimate LiDAR metrics (Shi et al. 2018), through which aspects of the vertical structure of the forest can be mapped.

Therefore, our study aims to examine 3D point clouds derived from UAV LiDAR to determine the winter wheat traits in the winter wheat field trial. Methodologically, we transfer the widely used LiDAR metrics in the forest sector to the analysis of crop traits. As a proof of concept, we analyse the data from a UAV LiDAR campaign in the growing season of 2020. We focus on five objectives:

- (i) Determine the absolute crop height from one UAV LiDAR campaign.

- (ii) Estimate wheat biomass and nitrogen uptake using crop height derived from UAV LiDAR and LiDAR metrics.
- (iii) Validate the results with manual height measurements.
- (iv) Validate the trait estimations and the height of the crop with the crop heights derived from SfM/MVS using UAV-RGB imagery.
- (v) Validate the estimated biomass and nitrogen uptake data against destructively sampled measurements.

## 2 Materials and Methods

### 2.1 Study Site and Field Sampling

The study site was situated on the Campus Klein-Altendorf (CKA, [www.cka.uni-bonn.de](http://www.cka.uni-bonn.de)), about 20 km southwest of Bonn. The region's climate is warm temperate with mild summers and winters and a mean temperature of 9.3 °C. The dominance of polar fronts leads to unpredictable weather with frequent cloud cover. The mean annual precipitation is about 600 mm, with precipitation relatively constant

throughout the year and a maximum in the summer months. Consequently, the region's climate is classified as warm temperate, fully humid with warm summer (Cfb) according to the Köppen–Geiger Climate Classification. Fertile soils and intensive agricultural use further characterise the region. The main crops grown are maize, sugar beet, barley, rape-seed, and wheat.

The studied winter wheat field trial (50°37'12" N, 6°59'50" E) was managed by the Institute of Crop Science and Resource Conservation (INRES, University of Bonn, Germany) (Fig. 1). It consisted of 120 plots arranged in five rows of 24, with each plot measuring 7 m × 1.5 m. There was one untreated buffer plot on the border of the field and two untreated plots between groups of treated plots to avoid border effects and mixing of nitrogen application. Each row contained three nitrogen treatments: 0, 120, and 240 kg ha<sup>-1</sup>, and each treatment was applied to six neighbouring plots. For each treatment of each row, the following six winter wheat cultivars were grown: Heines II, Heines VII, Heines Rot, Jubilar, Sperber, and Tommi.

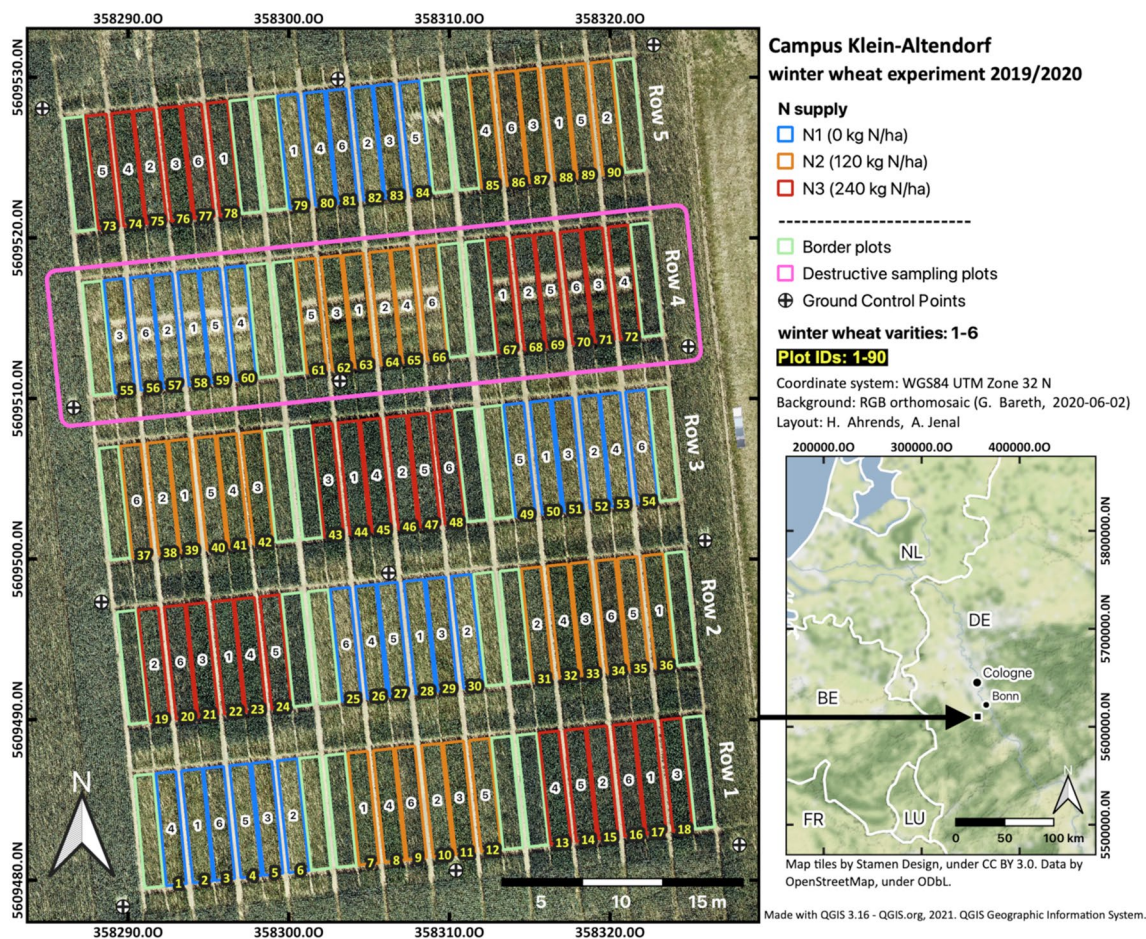


Fig. 1 Overview of the winter wheat field trial and location of the study site (Jenal et al. 2021)

The field measurements took place on April 8 and 28, May 13 and 26, June 9, and July 2, 2020. On these days, destructively sampling of biomass was performed at each of the 18 experiment plots in row four. Three by three rows of plants, each 50 cm long, were cut close to the ground with conventional garden shears. The biomass of each of the three rows was measured separately, for the analysis the mean of three measurements was used. Then, part of the 54 samples for each day were oven dried at 105 °C for 24 h to measure the plant dry biomass (DBM). Next, a portion of the biomass was further dried at 60 °C until no further decrease in sample weight was observed. This portion was then analysed for carbon and nitrogen concentrations using a C/N analyzer [EuroEA3000, EuroVector S.p.A. (Italy)].

In addition, the plant heights of all 90 plots considered in the experiment were measured manually. The buffer plots were again excluded. The height measurements were done unconventionally: First, a metre stick was held in the centre of the plot. The plants were then aimed from the further cross side of the plot. Finally, the measuring stick was aimed at the surface of the plant and the height visible on the stick was noted. Hence, those height measurements might be influenced by the size of the highest plants in the plot.

## 2.2 Data Acquisition and Structure from Motion (SfM) Analysis of Optical RGB Images using the Phantom 4 RTK UAV

A Phantom 4 RTK UAV (DJI, Shenzhen, China) was used on the following dates: March 26, April 7 and 28, May 13 and 26, June 2 and 1, July 1 and 21, 2020. The flights were conducted 25 m above the ground using a double grid lawn-mower pattern with 80% vertical and horizontal overlap. During approximately 20 min of flight time, about 400 photos with a 20 MP resolution were taken in Program Mode. A particularity of this system is the ability to correct estimates of the UAV position during the flight using GNSS correction data. This correction data were obtained from the DJI base station D-RTK 2, set up during each flight. As a result, the positional information of the obtained images has a vertical and horizontal accuracy of about 5 cm and 1 cm, respectively (DJI 2022).

To verify this high positional accuracy, 12 permanent ground control points (GCP's), each measuring 20 cm × 20 cm, were deployed. The positions of the markers were surveyed with a Topcon GR-5 positioning DGPS positioning system using a Base / Rover constellation with RTK correction.

The images taken by the UAV were analysed using the Structure from Motion (SfM) approach implemented in the software Metashape (Version 1.5.2, Agisoft LLC, St. Petersburg, Russia). Metashape allows a 3D reconstruction of the scene. First, image matching was performed on all images

from one date on the full resolution images with a key point limit of 1,000,000 and a tie point limit of 40,000. Next, a dense cloud with high quality was computed with the filtering intensity set to “aggressive” for the first date and “mild” for all later dates. The dense cloud in “high” setting was then used to create the digital elevation models (DEM) with a pixel spacing of 1.31 cm and a digital orthophoto (DOP) with a pixel spacing of 0.66 cm per pixel. The processing of the data from the P4 RTK campaign was performed on a higher-grade processing computer (Intel XEON CPU E5-2687 W v3, 256 GB RAM, 2×NVIDIA Quadro M4000 GPU) and lasted 5–6 h for each survey date.

The first DEM, from March 12, 2020, where the winter wheat plants were very small, was used as the ground model. The later DEMs are interpreted as crop surface models (CSM), as they represent the surface of the plants. The ground model was subtracted from all later CSMs to estimate crop height (CH) for all later dates (Bendig et al. 2013).

Based on the CSMs of the multitemporal P4 RTK data, season-long models were established. A linear model for DBM and a non-linear model for nitrogen uptake were created from six dates of destructive plant measurements and the corresponding P4 RTK-based crop height measurements. More details of these models are described in the study by Jenal et al. (2021).

The analysis based on the P4 RTK dataset taken on June 2 showed plant height values that were too low. The reason for that issue was the contribution of bottom points, triggered, most likely, due to unfavourable image acquisition conditions for SfM, with bright, direct sunshine and moderate winds during the flight. Instead, we interpolated the plant heights from the dates prior (May 25) and post (June 12), where such problems did not occur (Jenal et al. 2021).

## 2.3 UAV LiDAR System and Campaign

The UAV LiDAR system used in this study was a Riegl MiniVUX-1-UAV laser scanner mounted on a DJI Matrice 600 pro UAV with a take-off weight of about 11.2 kg (Fig. 2). The scanner can perform up to 100,000 measurements per second with an accuracy of 1.5 cm (Riegl 2022). In UAV laserscanning, the accurate determination of the UAV's position and orientation is crucial for the subsequent accuracy of the recorded data. Therefore, the system was equipped with a highly precise inertial measurement unit (IMU), the APX-15 IMU. It measures the orientation of the UAV at any given time and records GNSS data for geolocation. GNSS correction data are also necessary to calculate the UAV's position during the data acquisition in the postprocessing. These GNSS correction data were logged by a TOPCON GR-5 DGPS with RTK correction during the flight, which was positioned next to the field.



**Fig. 2** The system used in this study, which is a UAV DJI Matrice 600 pro, with a Riegl Mini-VUX-1 LiDAR scanner

Accordingly, using the APX-15 allows estimation of the position at a positional accuracy of 2–5 cm. Roll and pitch can be estimated with a precision of  $0.025^\circ$  and heading with  $0.08^\circ$  (Applanix, 2022).

The actual UAV LiDAR flight took place on June 2, 2020. The flight altitude was 40 m above ground, and the speed was  $5 \text{ m s}^{-1}$ . The total flight time was approximately 12 min using around 50% of battery charge. The field trial area of 0.2 ha was overflowed and scanned five times in approximately one minute (Fig. 3). To test the potential for scanning a larger area, any remaining flight time was used to scan approximately 16 ha around the trial site. The flight control software UgCS (Version 3.4. build 609) was running on a

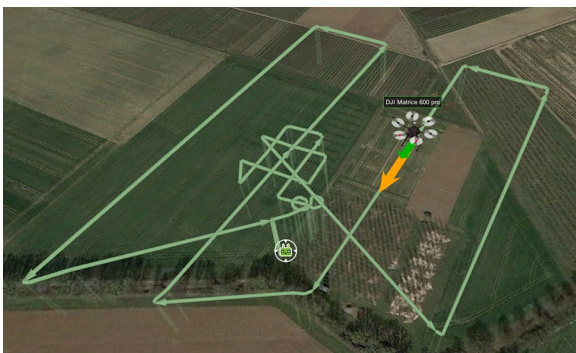


**Fig. 3** Flight plan of the UAV LiDAR campaign, June 2, 2020

laptop computer, which was connected to an Android tablet running the UgCS for DJI Android app (Version 2.17), which in turn was connected to the UAV flight controller. Thus, the UAV flight was completely automated.

## 2.4 Generating and Processing of the 3D UAV LiDAR Point Cloud

The first step to generate the 3D LiDAR point cloud is estimating the trajectory of the UAV, based on the data from IMU and the GNSS correction data. This step was carried out in the software POSpac UAV™ (Applanix, Richmond Hill, Ontario, Canada, Version 8.4., Service Pack1). The corrected trajectory was then imported into the RiProcess software (Version 1.9.2. RIEGL, Horn, Austria) to calculate the LiDAR point cloud. In a final step, the accuracy of the trajectory was further enhanced using RiPrecision (Version 1.9.2. RIEGL, Horn, Austria). In that step, spatial reference objects were included, extracted from the DOP from the optical UAV. The steps to generate the LiDAR point cloud were performed on a laptop computer without significantly strong hardware equipment (Intel Core i5 8350U processor, 8 GB RAM) in under 30 min.

The point density over the trial was approximately  $450\text{--}1250 \text{ points m}^{-2}$  and about  $100\text{--}150 \text{ points m}^{-2}$  in the area around the trial. A total of 2.3 million points were acquired over the trial, and 27.2 million total points (see Fig. 4).

The UAV LiDAR point cloud was analysed using LAS-Tools (Version: 210,720, rapidlasso GmbH, Gilching, Germany). First, outlier points were identified in the UAV LiDAR point cloud and removed as soon as five or fewer points were within one cubic metre. Next, only those points were further analysed, that either fell within the area of the plots or within the area that was to be harvested one week after the flight. All other points were excluded from further analysis. Out of the remaining points, the points representing the ground were classified using the lasground functionality of LASTools to normalise the height of the points from ellipsoidal absolute heights to the height above ground. The

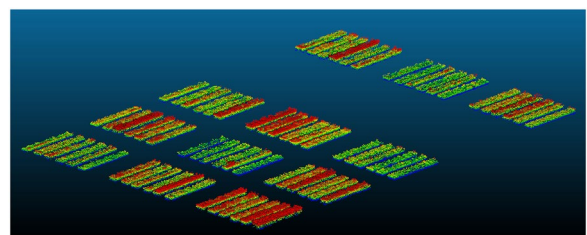


**Fig. 4** 3D view of the normalised point cloud of the 72 plots which were not destructively sampled, coloured by height (red: high crop height; blue: low crop height)

"lasground\_new" implementation was used with default values, but setting the offset value to 0. Finally, the point cloud metrics were calculated using the lascanopy functionality of LAStools. Those metrics have been successfully used as predictors in various LiDAR forest studies (Bouvier et al. 2015; Coops et al. 2021; Shi et al. 2018). However, we adopted the methodology to agricultural crops, as we set the height cut-off, typically used in forest studies to neglect smaller trees and bushes, to 0.

The following metrics were calculated based on the vertical distribution of the normalised point heights within each reference area (i.e. either plot or area to be harvested): average, maximum, percentiles (every 5%, plus 99%), the number of points in different height ranges (between 0 and 10 cm, 10 and 20 cm, 20 and 30 cm, 40 and 50 cm, 50 and 60 cm, 60 and 70 cm), and bincentiles (every 5 from 5 to 95) (Stefanidou et al. 2020). A bincentile is the percentage of points above a reference height, with the reference height being the percentage of the maximum height, which is added to the end of the bincentile. Bincentiles can be considered as a canopy density measure (Stefanidou et al. 2020). The measure of the return energy of the emitted laser beam is the basis for generating the LiDAR intensity, which RiProcess then uses to calculate the reflectance of each LiDAR point. Based on the reflectance of the points from each reference area (i.e. either plot or area to be harvested), we calculated the reflectance's average, standard deviation, and percentiles of the reflectance (25, 50, 75, 80, 85, 90, 95). Furthermore, the number of points per reference area and the Height of Median Energy (HOME) (Drake et al. 2002) were calculated. The HOME combines reflectance and height. For its calculation, all LiDAR points of a plot are first sorted by height, and then the height is determined where the sums of reflection of all points above and below are equal.

Based on these UAV LiDAR metrics, linear models with manually measured plant heights, data from optical UAV

flights, and destructive biomass data were established. We used the coefficient of determination ( $R^2$ ) and the root mean square error (RMSE) as statistical measures to evaluate the potential of the UAV LiDAR metrics.

### 3 Results

In Table 1, the relevant correlations and the sections, in which the respective results are presented, are shown. In all results chapters, we mainly focus on three metrics: the 95th percentile of the height, the bincentile 60, and the 90th percentile of the reflectance, as we see these three as the best representative of different categories of metrics with high correlations.

#### 3.1 UAV LiDAR Metrics are Correlated with Manually Measured Crop Heights

We first evaluated the UAV LiDAR point cloud data using a dataset of manual height measurements from the 72 winter wheat plots that were not sampled destructively. The metrics, which were derived for each plot, showed a moderate to strong linear correlation with the manual height measurements (Fig. 5). The metric showing the highest correlation was the 95th percentile of the normalised height ( $R^2 = 0.86$ ,  $p < 0.001$ , see Fig. 5) with an RMSE value of 4.1 cm. A lower correlation ( $R^2 = 0.61$ ,  $p < 0.001$ ) was observed for the manually measured plant height with the LiDAR metric bincentile 60. Interestingly, all unfertilised plots, and only one of the plots fertilised with 120 kg ha<sup>-1</sup>, have a bincentile 60 of more than 85%.

The 90th percentile of the LiDAR reflectance shows a moderate negative linear correlation ( $R^2 = 0.54$ ,  $p < 0.001$ ) with the manually measured plant heights. The RMSE is, with 7.5 cm, about twice as high as for the 95th percentile

**Table 1** Linear correlations ( $R^2$ ) of the UAV LiDAR metrics with the reference data of the present study

dependent variable	UAV LiDAR metric																							...	see figure described in section
	95 <sup>th</sup> percentile of the height	90 <sup>th</sup> percentile of the height	85 <sup>th</sup> percentile of the height	80 <sup>th</sup> percentile of the height	95 <sup>th</sup> percentile of the height	75 <sup>th</sup> percentile of the height	70 <sup>th</sup> percentile of the height	90 <sup>th</sup> percentile of the reflectance	65 <sup>th</sup> percentile of the height	95 <sup>th</sup> percentile of the reflectance	mean height	60 <sup>th</sup> percentile of the height	55 <sup>th</sup> percentile of the height	bincentile 60	50 <sup>th</sup> percentile of the height	85 <sup>th</sup> percentile of the reflectance	HOME	maximum height	bincentile 55	bincentile 70	45 <sup>th</sup> percentile of the height	40 <sup>th</sup> percentile of the height	no. of points 0-10 cm		
manually meas. plant height	0.86	0.84	0.84	0.83	0.86	0.82	0.81	0.54	0.80	0.46	0.79	0.79	0.78	0.61	0.77	0.58	0.76	0.82	0.60	0.58	0.75	0.74	0.47	5	3.1
P4 RTK plant height	0.92	0.92	0.91	0.90	0.89	0.89	0.88	0.63	0.87	0.57	0.86	0.85	0.84	0.71	0.83	0.66	0.83	0.82	0.71	0.64	0.81	0.80	0.64	6	3.2
DBM mod. by P4 RTK	0.92	0.92	0.91	0.90	0.89	0.89	0.88	0.63	0.87	0.57	0.86	0.85	0.84	0.71	0.83	0.66	0.83	0.82	0.71	0.64	0.82	0.81	0.64	7	3.3
nitrogen uptake mod. by P4 RTK	0.69	0.70	0.70	0.70	0.64	0.69	0.68	0.54	0.67	0.51	0.67	0.66	0.65	0.54	0.65	0.55	0.64	0.61	0.58	0.42	0.64	0.63	0.80	...	
destructively meas. DBM	0.63	0.66	0.67	0.68	0.55	0.68	0.68	0.74	0.68	0.68	0.68	0.67	0.67	0.80	0.69	0.77	0.69	0.40	0.78	0.71	0.68	0.69	0.45	8	3.4
destructively meas. nitrogen uptake	0.56	0.60	0.61	0.62	0.47	0.62	0.63	0.88	0.62	0.87	0.60	0.62	0.61	0.84	0.62	0.83	0.62	0.29	0.82	0.82	0.61	0.61	0.40		

← decreasing  $R^2$  (max per row) →

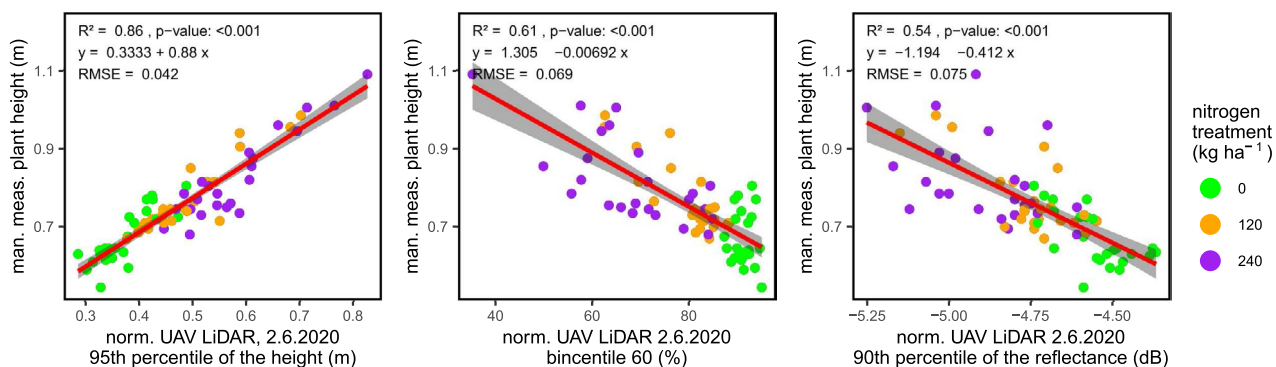


**Fig. 5** Linear correlation of the manual height measurements with the UAV LiDAR metrics. The grey area around the red regression line indicates the 95% confidence level interval

of the height. Especially the group with the highest fertiliser input (240 kg ha<sup>-1</sup>) shows high residuals. In general, only the height percentiles of the UAV LiDAR-derived heights are in great agreement with the manually measured heights. However, the ability of the bincentile 60 to separate the unfertilized group of plots from the rest of the plots is noteworthy.

### 3.2 UAV LiDAR Metrics are Correlated with the P4 RTK SfM Crop Heights

The correlations of the UAV LiDAR metrics with the crop heights from P4 RTK (Fig. 6) were similar to the correlations of the UAV LiDAR with the manual measurements (Fig. 5). However, these correlations are stronger in magnitude than those seen for the manual measurements. We observed the strongest correlation of P4 RTK-derived crop height with the UAV LiDAR metric 95th percentile of the height ( $R^2=0.92$ ,  $p < 0.001$ ,  $n = 72$ ), reaching an RMSE of only approx. 3 cm.

### 3.3 UAV LiDAR Metrics are Correlated with DBM and Nitrogen Uptake Modelled by P4 RTK SfM

The DBM modelled by the P4 RTK data showed the same strong correlation with the UAV LiDAR metrics data as the P4 RTK crop height alone ( $R^2=0.92$  for the 95th percentile of the height, 0.71 for the bincentile 60, and 0.64 for the 90th percentile of the reflectance).

The nitrogen uptake, on the contrary, was not modelled linearly, and therefore a slightly non-linear trend is observed in the comparison, leading to weaker linear correlations ( $R^2=0.69$  for 95th percentile of the height, 0.55 for the bincentile 60, and 0.55 for the 90th percentile of the reflectance). Yet, the three diagrams in the lower part of Fig. 6 show that there is also a relation of the LiDAR metrics to the modelled nitrogen uptake modelled by the optical system.

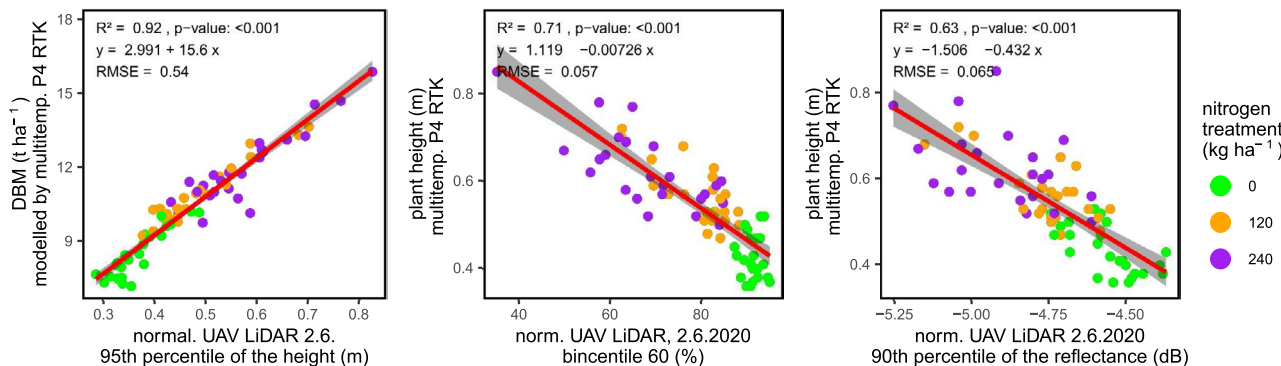


**Fig. 6** Linear correlations of the P4 RTK Crop Surface Height (CSH) measurements with the UAV LiDAR metrics. The grey area around the red regression line indicates the 95% confidence level interval

### 3.4 UAV LiDAR Metrics are Correlated with Destructively Measured DBM and Nitrogen Uptake

In the 18 destructively sampled plots, the dry biomass information and nitrogen uptake were destructively measured one week before (May 26) and one week after the UAV LiDAR campaign (June 9). The interpolated crop traits from those samplings could be related to the LiDAR height metrics from those areas that were harvested one week after the LiDAR campaign.

Remarkably, the bincentile 60 UAV LiDAR metric outperformed the average height in DBM as well as in nitrogen uptake estimation (Fig. 8). Especially encouraging is its very high correlation with nitrogen uptake ( $R^2=0.85$ ,  $p<0.001$ ). In general, we found a slightly higher correlation of UAV LiDAR metrics with the destructive samplings than in the analysis before, where P4 RTK-derived heights were used to model the crop traits.

## 4 Discussion

The present study's results demonstrate the possibility of estimating winter wheat crop traits from a single UAV LiDAR campaign using LiDAR metrics. Two main results

support that finding. First, we observed a high correlation of the UAV LiDAR data with the manual plant height measurements ( $R^2=0.86$ ,  $n=72$ ,  $p<0.001$ ). Second, we found a very high correlation of the LiDAR UAV data with the plant height measurements derived from the SfM analysis of the P4 RTK data ( $R^2=0.92$ ,  $n=72$ ,  $p<0.001$ ). This finding agrees with Bates et al. (2021), one of the few studies on the topic. Bates et al. (2021) also used the capability of UAV LiDAR to partially penetrate winter wheat and, thus, acquire a ground model and canopy information from a single UAV LiDAR observation. They used the resulting ground and canopy information to estimate the Leaf Area Index (LAI). However, we used the ground model to normalise all LiDAR points, enabling the computation of LiDAR metrics from the UAV LiDAR point cloud. Although these metrics were previously introduced in the context of forest inventory using LiDAR (Lim et al. 2003), they provided accurate predictions of winter wheat traits in our study. To the authors knowledge, the application of LiDAR forest metrics to derive crop traits has not been investigated before.

Based on the LiDAR metric 95th percentile of the height, the winter wheat plant heights were accurately estimated. We applied previously existing models from optical imaging UAV data and SfM analysis, which was performed season-long. In this way, we successfully established models for

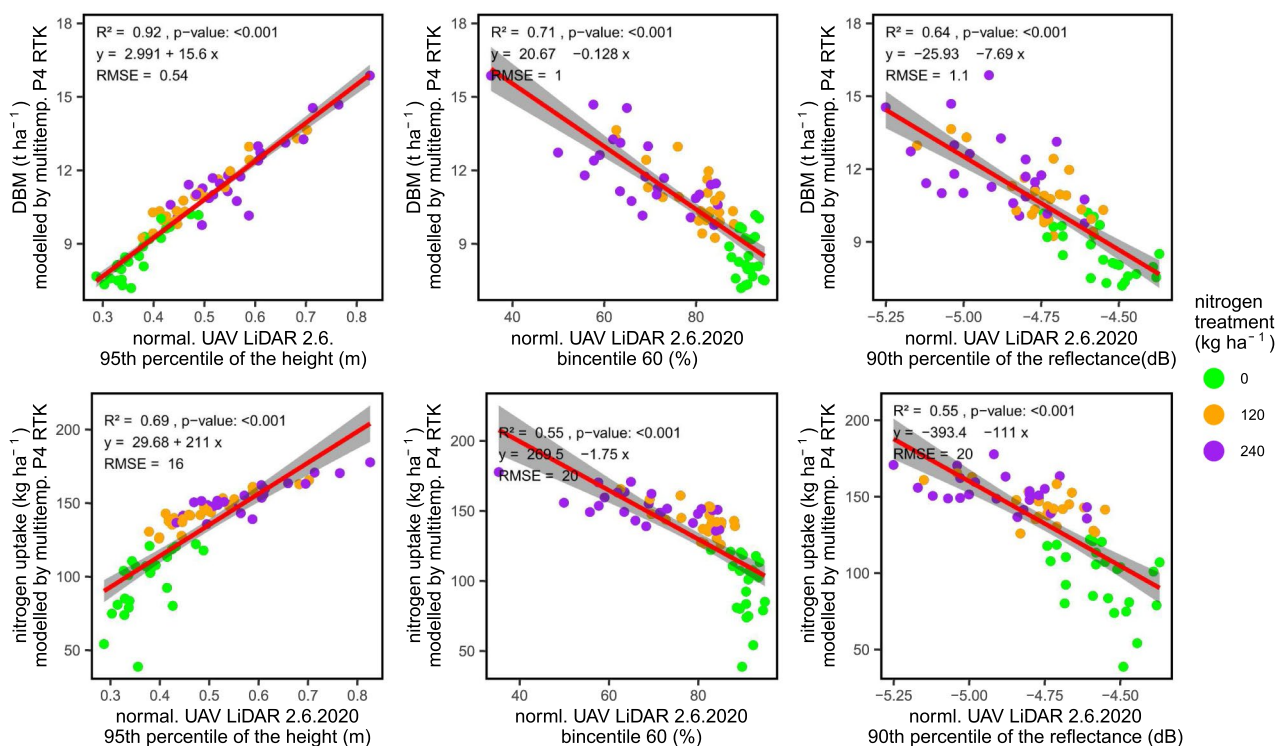


**Fig. 7** Linear correlations of the P4 RTK-derived crop trait measurements with UAV LiDAR metrics. The grey area around the red regression line indicates the 95% confidence level interval



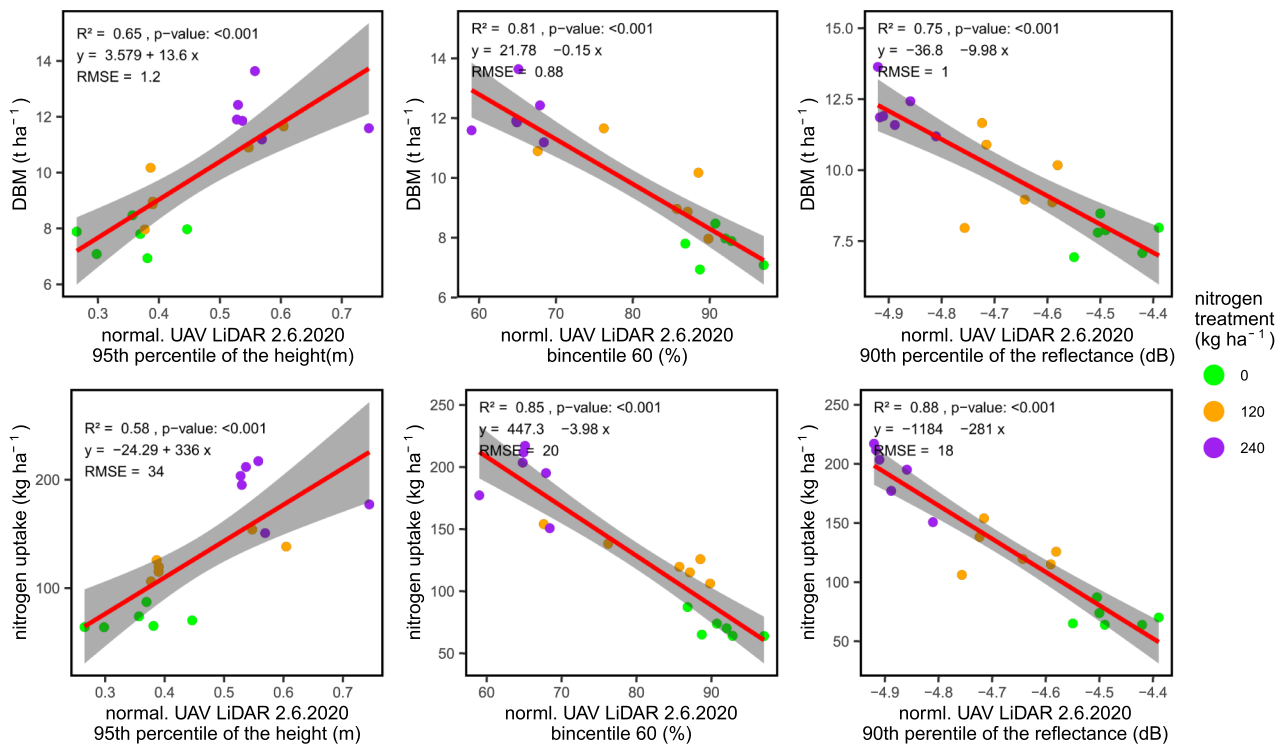


**Fig. 8** Linear Correlations of the destructive measurements with the UAV LiDAR metrics. The grey area around the red regression line indicates the 95% confidence level interval

DBM and nitrogen uptake for the 72 plots of the winter wheat field trial that were not destructively sampled. Those models show the same correlation as the models with the P4 RTK height. This is not surprising since the P4 RTK biomass estimation is also based on a linear model, with the P4 RTK-derived plant heights as input. However, the regression shown here indicates how the DBM can also be calculated from the LiDAR metrics. Those models created with the P4 RTK season-long observations were similar to those established with the 18 available destructive measurements. As shown in Figs. 6 and 7, the models for the DBM estimation, for example, are almost identical. The models for nitrogen uptake are also in the same range.

We argue that the potential of UAV LiDAR metrics for monitoring winter wheat extends to estimating other traits in addition to plant height. Of the 57 calculated UAV LiDAR metrics, we identified two metrics that estimated DBM from destructive sampling and nitrogen uptake variation with high accuracy. The first metric was the bincentile 60. It is calculated based on the vertical distribution of the LiDAR points. Of all metrics, it showed the strongest correlation with the destructively measured DBM ( $R^2 = 0.81$ ,  $P < 0.001$ ,  $n = 18$ ) (Fig. 8). Hence, we conclude that the bincentile 60 revealed parts of the structure of the winter wheat plants, especially plot canopy density, that are relevant for estimating DBM. The second metric was the 60th percentile of the

reflectance, which best described the variation in nitrogen uptake in the destructively measured samples ( $R^2 = 0.88$ ,  $P < 0.001$ ,  $n = 18$ ) (Fig. 8). Both LiDAR metrics, for DBM and nitrogen uptake, perform as good as optical estimators in the visible, near-infrared, and shortwave-infrared domain (VNIR/SWIR) as described by Jenal et al. (2021) for the same field experiment.

The LiDAR reflectance measures the amount of energy reflected to the sensor. Eitel et al. (2014) used a green Laser's reflectance to estimate winter wheat's nitrogen concentration. Hence, we expected that the reflectance could be used as a proxy for biophysical parameters of the winter wheat plants. Furthermore, the UAV LiDAR system of the present study works in the near-infrared region (809 nm), which is known from hyperspectral studies on winter wheat. For example, Wei et al. (2012) identified the wavelength region relevant for estimating leaf nitrogen accumulation. However, our expectation was not supported as we observed a negative correlation between the reflectance with DBM and plant height. We found that the LiDAR reflectance in our study was influenced mainly by interactions of the LiDAR with the ground, which has a higher reflectance than the plants. Hence, the higher reflectance of plots having plants of lower height and density is probably explained by the fact that more points originate from the ground because the LiDAR beam is more likely to reach the ground.

However, as the plants' density and height heavily influence the LiDAR reflection, the 90th percentile of reflectance was the most relevant LiDAR metric for approximating the nitrogen uptake of the winter wheat plants.

UAV LiDAR systems are still quite costly. Although a detailed cost–benefit analysis of UAV LiDAR is beyond the scope of the present study, we found a considerable gain in productivity. Compared to much cheaper ultrasonic devices, which only provide point measurements, the UAV LiDAR provides spatially continuous data and can survey much larger areas in a given time. Terrestrial LiDAR can only survey up to 20 ha per day. However, in this study, we acquired more than 16 ha with the UAV LiDAR in about ten minutes. Compared to SfM analysis, based on RGB images, UAV LiDAR benefits from two advantages. First, the flight time to capture the RGB images with the P4 RTK UAV was about 20 min, whereas it took only about one minute flight time to scan the area of the winter field trial. Second, SfM analysis of a single date required 5–6 h of computation time on a higher-grade computer, whereas LiDAR data can be made available within half an hour after the flight without significant processing. Additionally, for the LiDAR UAV approach, we presented in this study, only one UAV campaign is necessary. In contrast, in the case of optical imaging, an additional campaign to survey the ground is needed early in the growing season.

Our study presents a proof-of-principle based on data from a single UAV LiDAR flight. Furthermore, some conclusions are drawn on the basis of the analysis of 18 destructive measurements. Future studies should be based on a greater number of destructive measurements to replicate our findings. Moreover, winter wheat fields change dramatically during the growing season. The UAV LiDAR metrics that worked in our study might not be equally accurate in other growing stages or for the whole growing season. We could not determine which of the UAV LiDAR metrics performs optimally for time-series analysis. Therefore, the study should be repeated with more UAV LiDAR flights encompassing the whole growing period. Using datasets from different locations over several years should allow the established models to be validated and refined.

Another refinement results from deriving additional UAV LiDAR metrics used to predict winter wheat traits. The UAV LiDAR metrics calculated in this study are restricted to those implemented in the software LAsTools. However, LiDAR metrics can also be derived using other approaches (e.g. Hackel et al. 2016). In particular, the workflow presented in our study can be easily adapted to integrate more LiDAR metrics.

In this study, we investigated linear models. More sophisticated approaches such as multivariate models, machine learning or deep learning algorithms usually have a higher prediction accuracy and can be used to combine

several variables (i.e. metrics). However, we decided not to use these approaches for two reasons. First, our linear models and a resulting correlation coefficient for each LiDAR metric allowed us to demonstrate the different LiDAR metrics and their potential for estimating winter wheat crop traits. All regressions and data in this study are made freely available to allow replication of our results and comparison with future work. Second, machine learning approaches require independent test datasets to avoid overfitting, preferably from different growing seasons and multiple study sites.

Plant height is a proven proxy measure for DBM (Bendig et al. 2014; Tilly et al. 2014) and the vertical structure of plants can be used as a proxy for nitrogen uptake (Tilly and Bareth 2019). However, the correlation of plant height with nitrogen uptake is not as strong as that with DBM, as was also the case in the present study. We presented a workflow to calculate the height of the winter wheat plants. But more importantly, to derive additional information that is contained in the UAV LiDAR point cloud by adapting LiDAR metrics, which have previously been used in forest studies, for crop trait estimation. Based on this additional information from the UAV LiDAR metrics, we anticipate that a more accurate approximation of DBM, nitrogen uptake, and other traits of winter wheat crop should become feasible. Our approach could, of course, also be applied to other crops such as maize, barley, or rice. Furthermore, UAV LiDAR could be combined with other data for a more robust trait approximation, such as soil data (Argento et al. 2021) or multispectral imaging (Jenal et al. 2021).

Our findings may have implications for generating accurate and faster site-specific data for nitrogen fertilisation. The presented approach lends itself to several potential applications in precision agriculture. In conventional fields, polygon grids (Bareth et al. 2016) would have to be established to calculate the metrics. These grids would have a spatial resolution determined by the machinery performing the variable-rate nitrogen application. Such an approach could result in improved nitrogen fertilisation, thereby optimising yields and minimising environmental impacts. Our application of UAV LiDAR-derived metrics to the evaluation of crop traits in winter wheat illuminates the huge potential of this technology to advance research into other crops and in precision agriculture in general.

## 5 Conclusion

Plant height and structural characteristics are essential parameters in the non-destructive determination of plant traits. However, the established remote sensing for collecting plant structural data, such as SfM, ultrasonic devices, and conventional LiDAR (terrestrial and airborne), have

disadvantages that new UAV LiDAR systems can overcome. Therefore, this study aimed to demonstrate how single-date UAV LiDAR could be used to map winter wheat crop traits. We proposed using LiDAR metrics from LiDAR forest studies to calculate the crop traits. We demonstrated how the developed approach could successfully approximate plant height, DBM, and nitrogen uptake from a UAV LiDAR point cloud acquired over a winter wheat field trial. Further studies should aim to support our positive assessment over several years and repeated times during the growth period. Ideally, these studies would also include multi- and hyperspectral measurements with which the UAV LiDAR data could be combined and compared.

**Acknowledgements** We would like to acknowledge writing consultation provided by Brian Cusack during Science Craft's Online Writing Studio.

**Funding** Open Access funding enabled and organized by Projekt DEAL. This research was supported by Federal Ministry of Education and Research (BMBF) [Grant number 031B0734F] as part of the consortium research project "GreenGrass".

**Data availability** The datasets generated during and/or analysed during the current study are available from the corresponding author on reasonable request.

## Declarations

**Conflicts of Interest** The authors have no conflict of interest.

**Open Access** This article is licensed under a Creative Commons Attribution 4.0 International License, which permits use, sharing, adaptation, distribution and reproduction in any medium or format, as long as you give appropriate credit to the original author(s) and the source, provide a link to the Creative Commons licence, and indicate if changes were made. The images or other third party material in this article are included in the article's Creative Commons licence, unless indicated otherwise in a credit line to the material. If material is not included in the article's Creative Commons licence and your intended use is not permitted by statutory regulation or exceeds the permitted use, you will need to obtain permission directly from the copyright holder. To view a copy of this licence, visit <http://creativecommons.org/licenses/by/4.0/>.

## References

- Applanix (2022) APX-15 UAV *Datasheet*. [https://www.applanix.com/downloads/products/specs/APX15\\_UAV.pdf](https://www.applanix.com/downloads/products/specs/APX15_UAV.pdf). Accessed 7 Dec 2022
- Argento F, Anken T, Abt F, Vogelsanger E, Walter A, Liebisch F (2021) Site-specific nitrogen management in winter wheat supported by low-altitude remote sensing and soil data. *Precis Agric* 22(2):364–386. <https://doi.org/10.1007/S11119-020-09733-3/FIGURES/4>
- Bareth G, Bendig J, Tilly N, Hoffmeister D, Aasen H, Bolten A (2016) A comparison of UAV- and TLS-derived plant height for crop monitoring: using polygon grids for the analysis of crop surface models (CSMs). *Photogramme Fernerkundung Geoinform* 2016(2):85–94. <https://doi.org/10.1127/PFG/2016/0289>
- Barmeier G, Mistele B, Schmidhalter U (2016) Referencing laser and ultrasonic height measurements of barley cultivars by using a herbometre as standard. *Crop Pasture Sci* 67(12):1215–1222. <https://doi.org/10.1071/CP16238>
- Bates J, Montzka C, Schmidt M, Jonard F, Sensing (2021) Estimating canopy density parameters time-series for winter wheat using UAS Mounted LiDAR. *Remote Sens*. <https://doi.org/10.3390/rs13040710>
- Bendig J, Willkomm M, Tilly N, Gnyp ML, Bennertz S, Qiang C, Miao Y, Lenz-Wiedemann VIS, Bareth G (2013) Very high resolution crop surface models (CSMs) from UAV-based stereo images for rice growth monitoring in Northeast China. *Int Arch Photogramm Remote Sens Spat Inf Sci* 40:45–50. <https://doi.org/10.5194/isprsarchives-XL-1-W2-45-2013>
- Bendig J, Bolten A, Bennertz S, Broscheit J, Eichfuss S, Bareth G (2014) Estimating biomass of barley using crop surface models (CSMs) derived from UAV-based RGB imaging. *Remote Sens* 6(11):10395–10412. <https://doi.org/10.3390/RS61110395>
- Bouvier M, Durrieu S, Fournier RA, Renaud JP (2015) Generalizing predictive models of forest inventory attributes using an area-based approach with airborne LiDAR data. *Remote Sens Environ* 156:322–334. <https://doi.org/10.1016/J.RSE.2014.10.004>
- Coops NC, Tompalski P, Goodbody TRH, Queinac M, Luther JE, Bolton DK, White JC, Wulder MA, van Lier OR, Hermosilla T (2021) Modelling lidar-derived estimates of forest attributes over space and time: a review of approaches and future trends. *Remote Sens Environ* 260:112477. <https://doi.org/10.1016/J.RSE.2021.112477>
- DJI (2022) P4 RTK - Produktinformationen - DJI. <https://www.dji.com/de/phantom-4-rtk/info#specs>. Accessed 7 Dec 2022
- Drake JB, Dubayah RO, Clark DB, Knox RG, Blair JB, Hofton MA, Prince S (2002) Estimation of tropical forest structural characteristics using large-footprint lidar. *Remote Sens Environ* 79(2–3):305–319. [https://doi.org/10.1016/S0034-4257\(01\)00281-4](https://doi.org/10.1016/S0034-4257(01)00281-4)
- Eitel JU, Magney TS, Vierling LA, Brown TT, Huggins DR (2014) LiDAR based biomass and crop nitrogen estimates for rapid, nondestructive assessment of wheat nitrogen status. *Field Crop Res* 159:21–32. <https://doi.org/10.1016/j.fcr.2014.01.008>
- Gastal F, Lemaire G (2002) N uptake and distribution in crops: an agronomical and ecophysiological perspective. *J Exp Bot* 53(370):789–799. <https://doi.org/10.1093/JEXBOT/53.370.789>
- Hackel T, Wegner JD, Schindler K (2016) Contour Detection in Unstructured 3D Point Clouds. In: 2016 IEEE Conference on Computer Vision and Pattern Recognition (CVPR), 2016-December, 1610–1618. <https://doi.org/10.1109/CVPR.2016.178>
- Hansen PM, Schjoerring JK (2003) Reflectance measurement of canopy biomass and nitrogen status in wheat crops using normalized difference vegetation indices and partial least squares regression. *Remote Sens Environ* 86(4):542–553. [https://doi.org/10.1016/S0034-4257\(03\)00131-7](https://doi.org/10.1016/S0034-4257(03)00131-7)
- Heege HJ, Reusch S, Thiessen E (2008) Prospects and results for optical systems for site-specific on-the-go control of nitrogen-topdressing in Germany. *Precis Agric* 9(3):115–131. <https://doi.org/10.1007/S11119-008-9055-3/FIGURES/9>
- Hoffmeister D, Bolten A, Curdt C, Waldhoff G, Bareth G (2010) High-resolution Crop Surface Models (CSM) and Crop Volume Models (CVM) on field level by terrestrial laser scanning. In: Sixth International Symposium on Digital Earth: Models, Algorithms, and Virtual Reality, 7840, 78400E. <https://doi.org/10.1117/12.872315>
- Hoffmeister D, Waldhoff G, Korres W, Curdt C, Bareth G (2016) Crop height variability detection in a single field by multi-temporal

- terrestrial laser scanning. *Precis Agric* 17(3):296–312. <https://doi.org/10.1007/S11119-015-9420-Y>
- Huang S, Miao Y, Zhao G, Yuan F, Ma X, Tan C, Yu W, Gnyp ML, Lenz-Wiedemann VIS, Rascher U, Bareth G (2015) Satellite remote sensing-based in-season diagnosis of rice nitrogen status in Northeast China. *Remote Sens* 7(8):10646–10667. <https://doi.org/10.3390/RS70810646>
- Iqbal F, Lucieer A, Barry K, Wells R (2017) Poppy crop height and capsule volume estimation from a single UAS flight. *Remote Sens* 9(7):647. <https://doi.org/10.3390/RS9070647>
- Jenal A, Hüging H, Ahrends HE, Bolten A, Bongartz J, Bareth G (2021) Investigating the potential of a newly developed UAV-mounted VNIR/SWIR imaging system for monitoring crop traits—a case study for winter wheat. *Remote Sens* 13(9):1697. <https://doi.org/10.3390/rs13091697>
- Ju XT, Xing GX, Chen XP, Zhang SL, Zhang LJ, Liu XJ, Cui ZL, Yin B, Christie P, Zhu ZL, Zhang FS (2009) Reducing environmental risk by improving N management in intensive Chinese agricultural systems. *Proc Natl Acad Sci USA* 106(9):3041–3046. <https://doi.org/10.1073/PNAS.0813417106>
- Lemaire G, Jeuffroy MH, Gastal F (2008) Diagnosis tool for plant and crop N status in vegetative stage. Theory and practices for crop N management. *Eur J Agron* 28(4):614–624. <https://doi.org/10.1016/j.eja.2008.01.005>
- Li F, Miao Y, Hennig SD, Gnyp ML, Chen X, Jia L, Bareth G (2010) Evaluating hyperspectral vegetation indices for estimating nitrogen concentration of winter wheat at different growth stages. *Precis Agric* 11(4):335–357. <https://doi.org/10.1007/S11119-010-9165-6/FIGURES/3>
- Lim K, Treitz P, Wulder M, St-Onge B, Flood M (2003) LiDAR remote sensing of forest structure. *Prog Phys Geogr* 27(1):88–106. <https://doi.org/10.1191/0309133303pp360r>
- Mulla DJ (2013) Twenty five years of remote sensing in precision agriculture: Key advances and remaining knowledge gaps. *Biosys Eng* 114(4):358–371. <https://doi.org/10.1016/j.biosystemseng.2012.08.009>
- Niu Y, Zhang L, Zhang H, Han W, Peng X (2019) Estimating above-ground biomass of maize using features derived from UAV-based RGB imagery. *Remote Sens* 11(11):1261. <https://doi.org/10.3390/RS11111261>
- Pittman JJ, Arnall DB, Interrante SM, Moffet CA, Butler TJ (2015) Estimation of biomass and canopy height in Bermudagrass, Alfalfa, and wheat using ultrasonic, laser, and spectral sensors. *Sensors* 15(2):2920–2943. <https://doi.org/10.3390/S150202920>
- Riegl (2022) Miniaturized LiDAR sensor for unmanned laser scanning RIEGL miniVUX-1 UAV @. [www.ricopier.com](http://www.ricopier.com). Accessed 7 Dec 2022
- Schirrmann M, Hamdorf A, Giebel A, Gleiniger F, Pflanz M, Dammer KH (2017) Regression kriging for improving crop height models fusing ultra-sonic sensing with UAV imagery. *Remote Sens* 9(7):665. <https://doi.org/10.3390/RS9070665>
- Shi Y, Wang T, Skidmore AK, Heurich M (2018) Important LiDAR metrics for discriminating forest tree species in Central Europe. *ISPRS J Photogramm Remote Sens* 137:163–174. <https://doi.org/10.1016/J.ISPRSJPRS.2018.02.002>
- Stefanidou A, Gitas IZ, Korhonen L, Stavrakoudis D, Georgopoulos N (2020) LiDAR-based estimates of canopy base height for a dense uneven-aged structured forest. *Remote Sens* 12(10):1565. <https://doi.org/10.3390/RS12101565>
- ten Harkel J, Bartholomeus H, Kooistra L (2019) Biomass and crop height estimation of different crops using UAV-based lidar. *Remote Sens* 12(1):17. <https://doi.org/10.3390/RS12010017>
- Tilly N, Bareth G (2019) Estimating nitrogen from structural crop traits at field scale—a novel approach versus spectral vegetation indices. *Remote Sens* 11(17):2066. <https://doi.org/10.3390/RS11172066>
- Tilly N, Hoffmeister D, Cao Q, Huang S, Lenz-Wiedemann V, Miao Y, Bareth G (2014) Multitemporal crop surface models: accurate plant height measurement and biomass estimation with terrestrial laser scanning in paddy rice. *J Appl Remote Sens* 8(1):083671. <https://doi.org/10.1117/1.JRS.8.083671>
- Wei W, Xia Y, Tian YC, Liu XJ, Jun NI, Cao WX, Yan ZHU (2012) Common spectral bands and optimum vegetation indices for monitoring leaf nitrogen accumulation in rice and wheat. *J Integr Agric* 11(12):2001–2012. [https://doi.org/10.1016/S2095-3119\(12\)60457-2](https://doi.org/10.1016/S2095-3119(12)60457-2)
- Wilson TM, McGowen B, Mullock J, Arnall DB, Warren JG (2015) Nitrous oxide emissions from continuous winter wheat in the Southern Great Plains. *Agron J* 107(5):1878–1884. <https://doi.org/10.2134/AGRONJ15.0096>
- Zhang F, Hassanzadeh A, Kikkert J, Pethybridge SJ, van Aardt J, Ientilucci E, Renschler CS, Spacher PJ, Chowdhury S (2021) Comparison of UAS-based structure-from-motion and LiDAR for structural characterization of short Broadacre crops. *Remote Sens* 13(19):3975. <https://doi.org/10.3390/RS13193975>